LU-TP 22-07
February 2022

Geometry studies of high energy ^{16}O collisions

Aliaksei Kuzmenka

Department of Astronomy and Theoretical Physics, Lund University

Bachelor thesis supervised by Christian Bierlich

LUND
UNIVERSITY

Abstract

In this project a model of ^{16}O nuclei, where the nucleons are organised in α-clusters, was implemented in the Pythia Monte Carlo event generator. To study the effects of the new model, some observables, such as the distribution of the number of the wounded nucleons, charged particle multiplicity in the forward and central pseudorapidity region, and the pseudorapidity distribution for different centrality bins and eccentricity, are compared to the model originally implemented in Pythia (Woods-Saxon). Some basic theory that is used in the Pythia framework is also reviewed, as an amalgam from information taken from overview papers on the Glauber Model, Monte Carlo Event generators, the Angantyr model, and the string shoving model.

Populärvetenskaplig beskrivning

Collisions of matter (particles) sometimes happen naturally, and are sometimes performed in experiments, in order to investigate the fundamental properties of matter, such as its composition, or masses of the produced particles. One example of collisions happening naturally, is collisions of cosmic rays with the atmosphere of the Earth. The main participant of collisions of cosmics with the atmosphere is oxygen. It has been recently hypothesised that the oxygen nuclei have an unusual structure, in comparison to previously studied heavier nuclei.

At higher collision energy, smaller scales become more important. This means that more details of the internal structure are observed. The matter observed in our daily lives, consists of the atoms, which have a nucleus with electrons orbiting it. The nucleus in turn consist of nucleons: protons and neutrons. These particles, as well as other hadrons, are comprised of quarks, elementary particles, which have mass, electric charge, colour charge (called red, green or blue and respective anti-colours) and $\frac{1}{2}$-spin. These are intrinsic properties which determine how the particles interact. There are four fundamental forces: electromagnetic, weak, strong and gravity. Corresponding force carriers have been found for the first three. Particles that have electric charge may interact via the electromagnetic force by the exchange of photons. In the same way, the strong interaction affects particles with colour charge, the quarks. The branch of theoretical physics that studies the strong interaction is called Quantum Chromodynamics (QCD). The force carriers for the strong interaction, gluons, also possess a colour charge (carries both a colour and an anti-colour). That results in the strong force increasing in magnitude with the distance between the particles. It can be imagined as a string stretching between them. That analogy is the basis for the Lund String Model. If the energy stored in the string is large, it breaks by the production of a quark-antiquark pair. After the string breaks, there are two smaller pieces of string, with one quark from the original pair and one quark from the created pair at the ends of each string. The string may break down even further, and the resulting small string fragments are identified as hadrons, which are observed in the final state. This process is called string fragmentation and constitutes the model by which the hadrons are produced. In addition to this, strings can interact with each other. Strings will exert a repulsive force on each other, and the strength of repulsion decreases with the distance between the strings.

We return to the consideration of the collision itself. When two nucleons (or hadrons in general) collide at high energy, their constituents, quarks, can exchange gluons and be knocked out. That causes the string to stretch. Several strings can form simultaneously. This happens in particular in collisions of nuclei, when several nucleons participate. As was stated earlier, the strength of interaction between the strings depends on the distance between them. The internal nucleus geometry is therefore an important factor in determining the properties of the resulting hadrons. This means that an up-to-date structure for oxygen should be used in the models underlying simulations of collisions, in order to

correctly predict the experimental results. That is precisely the concern of this project: to implement an up-to-date geometrical model of oxygen in the simulation framework called Pythia.

The model of oxygen currently used within Pythia, has nucleons distributed according to a Woods-Saxon distribution. In the Woods-Saxon model, the density of nucleons depends only on the distance from the centre. The majority of nucleons are bunched up close to the centre of the nucleus, with the density dropping further from the centre. In the new model, there are four distinct clusters of four nucleons (two protons, two neutrons), with their centres located at the vertices of a tetraeder. The coordinates of nucleons within each cluster are distributed according to a Gaussian distribution.

Contents

1 Introduction

High energy collisions of matter can give insight into its properties. For example, at LHC, high energy ion collisions are studied in order to help test different hypotheses in QCD (as well as in other branches of theoretical physics). Collisions also sometimes happen naturally. The branch of physics that constantly deals with that is cosmic ray physics. Cosmic rays are high-energy radiation from outside the solar system, which, entering the atmosphere, start to collide with atmospheric particles, forming particle showers. One of the most predominant collision types is cosmic rays against oxygen, ^{16}O. Recently the hypothesis that ^{16}O might have a significantly different structure than heavy nuclei, which were previously studied at LHC, has been discussed [1]. So, it was decided to dedicate one of the runs of LHC to ^{16}O^{16}O collisions [2] in 2025. Besides studying the collisions in order to help answer some questions from cosmic ray physics (for example, the muon deficit in simulations in comparison to the measurements, called the Muon Puzzle), it also gives a good opportunity to observe the effects of different geometries on the final state.

To study the properties of the collisions, simulations are often used. Simulations can for example be used to calculate the background to a desired signal process, or to generate simulated events based on existing theory and experiments, to project the impact of additional experimental statistics. There are several frameworks for different purposes. One of them is called GLISSANDO [3], which stands for "GLauber Initial-State Simulation AND mOre". It is mostly used for calculating the initial states of ion collisions using the Glauber Model. Another simulation framework is the event generator Pythia [4]. It is a general purpose Monte Carlo event generator, which is equipped with a full particle production model. Such generators can output simulated data which looks more or less like what is seen at LHC experiments. This is exactly the type of generator which is useful for generation of backgrounds, or any other purpose that requires estimates of the final state of collisions. It is therefore important to update the simulations with new models when a new theory comes out.

A special feature of the ^{16}O structure is that, based on the nuclear lattice effective field theory [5], positions of nucleons in the nucleus are correlated. They are clustered in groups of two neutrons and two protons, effectively forming an α-particle. A model that reproduces that structure has been already implemented in GLISSANDO [3]. Having taken inspiration from GLISSANDO, the aim of this project is to implement a similar model in Pythia. The newly implemented model is then compared to the already existing model in Pythia, by considering some observables that are often used in real experiments.

In the theory part (Section 2) of this project report, general concepts and elements of the Pythia framework, namely the Glauber model (Subsection 2.1) and the particle production model (Subsection 2.3), will be introduced. In the following part (Section 3), the oxygen structure will be introduced, and the implemented model explained, along with some implementation details. Finally, in the results (Section 4), some measured quantities will be presented and compared with the existing implementation of the oxygen nuclear geometry

in Pythia.

2 Theory

In this part the main theory will be presented. Since the project is based on the Pythia [4] framework, some basic parts of it will be introduced in the beginning. Namely sections 2.1 and 2.3 address the parts of the framework that deal with the initial state and particle production in the simulations respectively. In section 2.2 the model currently used for oxygen collisions in Pythia will be briefly described. In the last section 2.4 the main observables used in this project will be introduced.

2.1 Glauber Model

The considerations made in this part of the theory follow the ones that are given in the Glauber model review in ref. [6].

The Glauber model is a model used to determine collision parameters, for example the number of collisions (N_{coll}) and number of participating nucleons (N_{part}), the latter with which the number of produced particles scales.

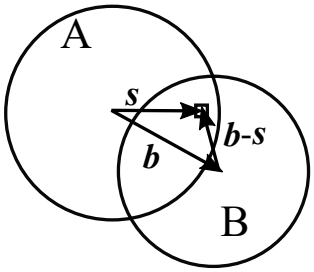

Figure 1: A depiction of two colliding nuclei: target A and projectile B. The centre of B is shifted by impact parameter $\boldsymbol{b}$ from A.

The Glauber model requires some parameters as an input, such as probability density function for the nucleon positions (normalised to one), $\rho(\boldsymbol{r})$, inelastic nucleon-nucleon cross section σ_{inel}^{NN} (in this project absorptive, or non-diffractive, interactions will be considered, i.e. interactions between nucleons happening only by exchange of gluons) and the impact parameter. In the Glauber model, collisions of nuclei are viewed in terms of individual interactions between nucleons. It is assumed that nucleons move in independent linear trajectories (eikonal approximation).

Let there be two colliding ions: target, A, and projectile, B, with the centre of B shifted by an impact parameter $\boldsymbol{b}$ from the centre of A (Figure 1). Let $T(\boldsymbol{s})$ be the nucleon distribution per unit transverse area, at a point displaced by $\boldsymbol{s}$ from the centre of a nucleus (at relativistic speeds the nuclei are contracted in the z direction, along the beam axis, meaning that they can effectively be treated as flat disks; $T(\boldsymbol{s})$ can also be obtained by integrating the probability density function of the nucleon distribution, $\rho(\boldsymbol{r})$, along the z axis).

Then, the probability of nucleons being in an overlapping area d^2s both for target and the projectile is

$$T_A(\boldsymbol{s})T_B(\boldsymbol{s}-\boldsymbol{b})d^2s. \tag{2.1}$$

Integration of this expression over all $\boldsymbol{s}$ gives a "thickness function",

$$T_{AB}(\boldsymbol{b}) = \int T_A(\boldsymbol{s}) T_B(\boldsymbol{s} - \boldsymbol{b}) d^2 s, \tag{2.2}$$

and by multiplying T_{AB} with the nucleon-nucleon inelastic cross-section, σ_{inel}^{NN}, (elastic interactions are not considered in this calculation, since they do not produce particles) one gets the probability for a given nucleon-nucleon interaction. With that, the probability of exactly n interactions is given by a binomial distribution:

$$P(n, \boldsymbol{b}) = \binom{n_A n_B}{n} \Big(T_{AB}(\boldsymbol{b}) \sigma_{inel}^{NN} \Big)^n \Big(1 - T_{AB}(\boldsymbol{b}) \sigma_{inel}^{NN} \Big)^{n_A n_B - n}, \tag{2.3}$$

with n_A and n_B being the number of nucleons in the target and the projectile respectively. In equation (2.3) the second term represents the probability of n specific interactions, the last term gives probability of the remaining $n_A n_B - n$ interactions not happening (due to unitarity of the probability), and the binomial coefficient in front gives the number of ways n interactions can happen from the total number of possible interactions between nucleons of the target and the projectile, $n_A n_B$.

One of the important observables is the number of collisions. Its expectation value $N_{coll}(\boldsymbol{b})$, which depends on the impact parameter, can be found as follows:

$$N_{coll}(\boldsymbol{b}) = \sum_{n=1}^{n_A n_B} n P(n, \boldsymbol{b}) = n_A n_B T_{AB}(\boldsymbol{b}) \sigma_{inel}^{NN}. \tag{2.4}$$

To find the expectation value for the number of participants, or wounded nucleons, it is important to state that the probability per unit area of at least one interaction of a target nucleon with any nucleon of the projectile, per unit area displaced by $\boldsymbol{s}$ from the centre of the target, is

$$T_A(\boldsymbol{s}) \Big(1 - \big(1 - T_B(\boldsymbol{s} - \boldsymbol{b}) \sigma_{inel}^{NN} \big)^{n_B} \Big), \tag{2.5}$$

where the term $\big(1 - T_B(\boldsymbol{s} - \boldsymbol{b}) \sigma_{inel}^{NN} \big)^{n_B}$ represents failure to interact with all projectile nucleons. Subtracting it from one gives the probability to interact with at least one nucleon, due to the unitarity of the probability. Thus, the expectation value for the number of participants, $N_{part,A}(\boldsymbol{b})$, of the target is

$$N_{part,A}(\boldsymbol{b}) = n_A \int T_A(\boldsymbol{s}) \Big(1 - \big(1 - T_B(\boldsymbol{s} - \boldsymbol{b}) \sigma_{inel}^{NN} \big)^{n_B} \Big) d^2 s, \tag{2.6}$$

and, similarly, the expression for the number of projectile participants, $N_{part,B}(\boldsymbol{b})$, follows:

$$N_{part,B}(\boldsymbol{b}) = n_B \int T_B(\boldsymbol{s} - \boldsymbol{b}) \Big(1 - \big(1 - T_A(\boldsymbol{s}) \sigma_{inel}^{NN} \big)^{n_A} \Big) d^2 s. \tag{2.7}$$

The total number of wounded nucleons is the sum of two values above:

$$N_{part}(\boldsymbol{b}) = N_{part,A}(\boldsymbol{b}) + N_{part,B}(\boldsymbol{b}). \tag{2.8}$$

In a Monte Carlo approach, these quantities are evaluated by simulating individual collisions one by one in "events". The nuclei are assembled by generating the positions of n_A and n_B nucleons according to given distributions for target and projectile respectively. The impact parameter is also generated randomly. There are different ways to consider when two nucleons will interact. The simplest way, is to consider an interaction to have happened when the distance between the nucleon centres, d, in the transverse plane (orthogonal to the beam axis), satisfies $d \leq \sqrt{\sigma_{inel}^{NN}/\pi}$, a so-called black disk model. The Monte Carlo approach is used in event generators, since observables useful in the experiment, such as charged particle multiplicity, cannot be calculated based on physics models directly from the output of a Glauber calculation (or it is extremely hard to do).

2.2 Large nuclei: The Woods-Saxon distribution

In large nuclei the interaction between the nucleons can be well described by a mean field potential which is significantly greater than the short-distance nucleon correlations. By default, in the Angantyr model, nucleons have a radially symmetric density distribution, the so-called Woods-Saxon distribution

$$\rho(r) = \frac{\rho_0}{1 + \exp\left(\frac{r-R}{a}\right)}. \tag{2.9}$$

Here r is the distance from the centre of the nucleus, ρ_0 is the density of the nucleons at $r = 0$, R is the radius at half-density and a is the skin width. On Figure 3b, 1600 points (in the xy plane) generated from a Woods-Saxon distribution are shown. For small and medium sized nuclei, such as ^{16}O, that description would not work. That follows from the fact that the contribution from the short-distance nucleon correlations becomes comparatively more significant. In Section 3 the case of ^{16}O will be discussed more.

2.3 Particle Production in the Angantyr Model

This section concerns the ideas presented in the papers "The Angantyr model for Heavy-Ion Collisions in PYTHIA8" [7], "General-purpose event generators for LHC physics" [8] and "Setting the string shoving picture in a new frame" [9].

In the majority of event generators used for studying *pp* collisions (such as Pythia), events are simulated using perturbative QCD and hadronization models. Such event generators achieved precise descriptions of the patterns observed in *pp* collisions. In the field of heavy ion collisions, however, the models usually rely on Quark–Gluon Plasma (QGP) formation

and hydrodynamic modeling (the basic idea is presented in Subsection 2.4 when discussing the connection between the eccentricity and the flow coefficients). Some features of the QGP were observed in *pp* collisions (such as enhanced production of hadrons containing strange quarks). That might mean that the dynamics of both systems are similar. In case the QGP is formed even in *pp*, then the effects should be included in the simulations. Otherwise, if the effects in *pp* collisions have a different origin, it might be possible to reproduce the observations made in nuclear collisions by stacking *pp* collisions on top of each other. The Angantyr model was created assuming the second possibility. It extrapolates the *pp* dynamics to pA and AA collisions through the following steps.
First, the positions of the nucleons are determined and the number of participating nucleons is estimated. This is achieved by using Glauber Monte Carlo simulations. Then contributions to the final state from every nucleon are estimated using the Pythia multi-parton interaction machinery. Then the final state is hadronised using the string fragmentation model.

2.3.1 Multi-Parton Interaction

The minimal production time τ_0 of a particle, in the frame in which it has only transverse momentum, is proportional to the inverse of its transverse mass, $m_\perp$ (let $m_\perp^2 = m^2 + p_\perp^2$ be the transverse mass, where m is the mass of a particle and $p_\perp$ is its transverse momentum): $\tau_0 \propto 1/m_\perp$. In the lab frame, this time is $\tau \propto \gamma\tau_0 = \cosh y/m_\perp$, where γ is a Lorentz factor and y is the corresponding rapidity (Section 2.4). If it moves with velocity v, the resolvable length scales are greater than or equal to $v\tau = \sinh y/m_\perp$. If $p_\perp$ is not too large (it applies for the majority of the produced particles) individual collisions can not be resolved, so it is safe to assume that the number of produced particles scales with the number of participants. Each wounded nucleon contributes approximately one half of the amount of particles produced in a *pp* collision, since a *pp* collision has two wounded nucleons. The number of produced particles in the final state, therefore scales roughly as $(N_{part}^A + N_{part}^B)/2$. At high $p_\perp$, on the other hand, the multiplicity scales with the number of collisions, N_{coll}, which satisfies $N_{coll} \geq (N_{part}^A + N_{part}^B)/2$.

This argument roughly states that final state multiplicity scales with the number of wounded nucleons according to some emission function, $F(\eta)$, which depends on pseudorapidity, η (a representation of an angle between the particle and the beam axis, more in the Subsection 2.4):

$$\frac{dN}{d\eta} = N_{part}^B F(\eta) + N_{part}^A F(-\eta). \tag{2.10}$$

In a wounded nucleon model $F(\eta)$ is obtained from data. In the Angantyr model, however, the emission function is dynamically generated using the multi-parton interaction (MPI) model in Pythia.

It is therefore necessary to introduce the way MPI events are handled in *pp* collisions in Pythia. As a first approximation all partonic sub-collisions are treated as almost un-

correlated QCD $2 \to 2$ scatterings. At low transverse momentum, $p_\perp$, the cross-section of interaction diverges within perturbative QCD, so, in Pythia, it is regulated using a parameter $p_{\perp 0}$:

$$\frac{d\sigma_{2\to 2}}{dp_\perp^2} \propto \frac{\alpha_S^2(p_\perp^2)}{p_\perp^4} \to \frac{\alpha_S^2(p_\perp^2 + p_{\perp 0}^2)}{(p_\perp^2 + p_{\perp 0}^2)^2}. \tag{2.11}$$

It is used to calculate the probability of additional partonic sub-scatterings.

If the model in which sub-scatterings are completely uncorrelated was used, particle production over the whole rapidity range in additional sub-scatterings would be allowed (Figure 2a left diagram). That would make it impossible to reproduce the data. Instead, the model in Pythia is modified such that the majority of additional, soft sub-scatterings can be colour-connected (connected by the colour lines) to partons produced in previous sub-scatterings. This process is known as colour reconnection (Figure 2a right diagram).

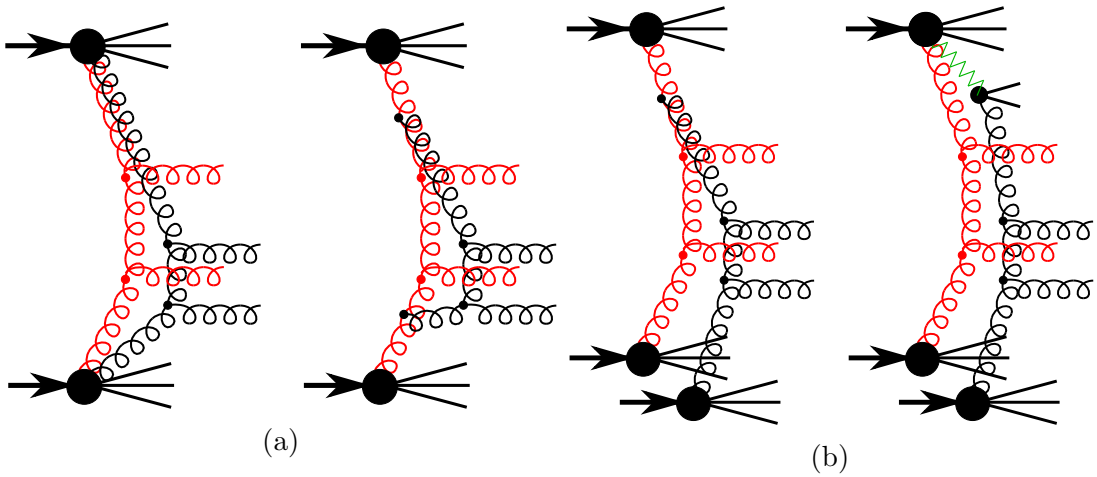

Figure 2: The figure (a) shows a schematic depiction of MPIs in a pp collision. The y-axis loosely represents rapidity: the higher the particle on the diagram, the higher rapidity it has, with zero in the middle and negative rapidity in the bottom part of the diagram. On the first diagram of the figure (a) colour lines of both sub-scatterings stretch over the whole rapidity region between the proton remnants. On the second diagram of (a) the additional sub-scatterings are colour-connected to the primary sub-scattering. The figure (b) shows the MPIs in a pA collision. The left diagram on the figure (b) represents how the secondary interaction is connected to the second nucleon and on the right diagram the secondary interaction is changed to a single-diffractive sub-scattering. (figures drawn from ref. [7], p.15 and p.17)

Taking the case of pA collisions, let the projectile proton interact with two nucleons in the target nucleus. Repeating the idea from pp collisions, instead of two separate sub-scatterings, there is a primary scattering of the projectile with one of the target nucleons, and an additional secondary sub-scattering with the second nucleon (Figure 2b left diagram). The same colour topology (consequently, the produced particle distribution)

would be obtained if the second sub-scattering would be a separate single-diffractive sub-scattering. When particles interact single-diffractively, one of the particles interact through the exchange of a colour singlet called a Pomeron, and the other one breaks down producing particles in only one hemisphere of the detector. Pythia has the machinery to handle such events as a Pomeron-proton collisions, but it was modified to reproduce the particle distribution in non-diffractive pp collision (Figure 2b right diagram). And thus, this can be extended to AA collisions.

2.3.2 Hadronization

Hadronization refers to a method used to transform coloured particles in the final state to the colourless hadrons ([8], p. 84.). This transition cannot be calculated from first principles (non-pertubative QCD is not solved and the case inherently can not be treated by lattice QCD without dynamical quarks), but some models were developed to reproduce realistic jets. In Pythia the Lund string model is used (the reviews for the model can be found in refs. [8], [9] and references therein).

It is easiest to illustrate the model by imagining a quark-antiquark pair, $q\bar{q}$, moving away from each other. One of the assumptions of the string model is that the Coulomb term in the interaction can be neglected (at large distances it becomes small and in overall it does not significantly change the hadron production pattern). As such, when the $q\bar{q}$-pair is produced, and the quarks move apart, a colour flux tube is stretched between them with a potential linear in the distance between the quarks. This result is also corroborated by lattice QCD (assuming that the tube is uniform along its length). The energy flow in such a system can be approximately described using the dynamics of a relativistic one-dimensional (without transverse extension) massless string. Such a description is Lorentz covariant. Let the quarks, $q\bar{q}$, move apart along the z axis. Then, the potential energy stored in the string, $V(r) = \kappa r$ with string constant κ (approximately 1 GeV/fm), increases. As a result, another pair of quarks $q'\bar{q}'$ may be produced, breaking the string and creating two separate colour-singlet systems: $q\bar{q}'$ and $q'\bar{q}$. Since quarks have mass, m, and transverse momentum, $p_\perp$, they should classically be created some distance apart, since the energy of the field between them is transformed into mass. Thus, when the pair $q'\bar{q}'$ is created in one point, the quarks tunnel out to the classically allowed region. The tunneling probability depends on $m_\perp$, and it is proportional to a Gaussian:

$$\exp\big(-\pi m_\perp^2/\kappa\big) = \exp\big(-\pi p_\perp^2/\kappa\big)\exp\big(-\pi m^2/\kappa\big). \tag{2.12}$$

One should note that the simple $q\bar{q}$ string does not have transverse excitations, so the $p_\perp$ of the quarks from the produced pair compensate each other. From factorisation of terms in Equation (2.12) it follows that the distribution of quark transverse momenta also follows a Gaussian distribution independently of flavour (the results slightly deviate from the experiment due to soft-gluon radiation). When the quarks organise into a hadron, the transverse momentum of the produced hadron gets contribution from all partons that

constitute it. The other term in equation (2.12) shows that the production of heavy quarks is suppressed. In fact, the production of charm and bottom quarks from hadronization is neglected in Pythia.

Further breaks of the string may happen if the invariant mass of the systems created is large enough. The string pieces created in the break must be on the mass shell to make a hadron, i.e. satisfy $m_\perp^2 = m^2 + p_\perp^2 = E^2 - p_z^2 = \kappa^2((\Delta z)^2 - (\Delta t)^2)$ where Δz and Δt is the distance between the vertices at which the string breaks (the hadron is formed between these vertices) in Minkowski space. The breaks are space-like separated, meaning that they are causally independent and can follow in any order. This gives rise to the "left-right symmetry", and a fragmentation function, $f(z)$, which describes how the energy is distributed among the produced hadrons, follows.

Baryon production can be explored using the "popcorn" model (the review can be found in ref. [8], p. 91), in which they appear due to successive creation of several $q'\bar{q}'$ pairs. A pair $B\bar{B}$ of baryons can be produced in the same general way as described before, but instead with creation of a diquark-antidiquark pair. The diquark-antidiquark pair does not appear as a single excitation, but the soft chromoelectric field treats the diquark as a single unit. Due to uncertainty in the diquark masses, their production can not be explored directly using tunneling. Also it is possible that mesons are created between the baryons: $BM\bar{B}$, or $BMM\bar{B}$, etc. In such cases the baryons share quarks from only one pair. In Pythia chains longer than $BM\bar{B}$ are neglected (so at most one meson can be created between a $B\bar{B}$ pair).

It would also be informative to look at tri-jet events, where a pair of quarks, as well as a gluon are produced, $q\bar{q}g$. The quarks at the endpoints of the strings carry one colour. The gluon carries both a colour and an anti-colour, so the string can be stretched from one quark via the gluon to the other quark. The gluon then can be treated as a kink on the string, carrying energy and momentum. In an event with several gluons they appear just as more kinks on the string. Emission of collinear or soft gluons have little effect on the string motion and fragmentation, which means that the model is collinear and infrared safe and that the lower cut-off scale for the parton shower does not significantly impact the string shape.

So far fragmentation of only one string was discussed here. MPIs may cause events where several strings are overlapping in the same region of space. As a cursory example let us consider the interaction between two parallel strings ([9], p.14). It works well as an approximation of the interaction between the strings in the case when only soft gluons are emitted (meaning that the strings stay parallel to each other along their length). Now the radius, R, of a string should be introduced instead of keeping it one-dimensional. From lattice QCD calculations, the colour-electric field is well approximated by Gaussian:

$$E = N \exp\big(-\rho^2/(2R^2)\big), \tag{2.13}$$

where ρ is the radius in cylindrical coordinates and N is a normalisation constant. The energy in the field per unit length is given by $\int d^2\rho E^2/2$. N is obtained by adjusting

the energy to a given fraction, g, of κ. That gives $N^2 = 2g\kappa/(\pi R^2)$. R and g are kept as tunable parameters. The energy per unit length from both strings is then given by $\int d^2\rho(E_1 + E_2)^2/2$. Let the strings be separated by distance d. The interaction energy is then equal to $2\kappa g \exp\big(-d^2/(4R^2)\big)$. The force per unit length, $f(d)$, can be obtained by taking the derivative of the last expression with respect to d:

$$f(d) = \frac{g\kappa d}{R^2} \exp\big(-d^2/(4R^2)\big). \tag{2.14}$$

It was here assumed that the colour flux tubes are oriented in the same direction, which leads to a repulsion between them. If the triplet fields are oriented opposite to each other, one gets either an octet field, which also gives repulsion, or sometimes a singlet field, which would cause attraction. In the latter case the strings are instead removed using colour reconnection.

This type of interaction between strings is known as the string shoving model. From the expression (2.14) it is clear that the strength of the interaction depends on the distance between the strings. That presents the argument for why the nuclear geometry is important.

2.4 Observable definitions

Rapidity, y, is a representation of a Lorentz boost γ. The relation is $\gamma = \cosh y$. In experimental particle physics the definition is modified, however:

$$y = 1/2 \ln \frac{E + p_z c}{E - p_z c}, \tag{2.15}$$

which is a representation of the Lorentz boost which takes the observer from the lab frame, to the frame in which the the particle observed has only transverse momentum, $p_\perp$. The longitudinal momentum p_z in Equation (2.15) is the momentum of the particle along the beam axis.

In connection to rapidity, pseudorapidity, η is used to describe the position of a particle in the detector. It represents the angle between the particle and the beam axis and is defined as in Equation (2.16):

$$\eta = -\ln\Big(\tan\big(\theta/2\big)\Big) = 1/2 \ln \frac{|\boldsymbol{p}| + p_z}{|\boldsymbol{p}| - p_z}, \tag{2.16}$$

where θ is the angle between the beam axis and the momentum of the particle. Pseudorapidity, unlike rapidity, does not depend on the energy of the particle, but only on its azimuthal angle. For massless particles pseudorapidity and rapidity are the same.

As was stated earlier, the number of particles produced in a collision scales with the number of wounded nucleons. The number of wounded nucleons also increases when the collision

is more central (the nuclei collide with smaller impact parameter). Thus, the charged particle multiplicity in the forward direction (at high η, in the case of this project taken to be $3.5 < \eta < 5$) monotonically depends on the impact parameter. This observable therefore provides a good basis for classifying the collisions by their centrality. This leads to the commonly used classification scheme for events, known as centrality binning. The distribution of particles produced in the forward direction is divided into percentiles, each representing a centrality bin, and events are classified according to those.

It is interesting to look at the pseudorapidity distribution of the produced particles. The distribution in η will be different for different centrality bins, since the multiplicity depends on the number of participants (as mentioned above), and the number of participants monotonically depends on the impact parameter (and consequently centrality) of the collision.

Besides that, the shape of the fireball (i.e. the collision region) produced in the collision also depends on the impact parameter. The shape is characterized by an observable called eccentricity. Eccentricity, ϵ_n, can be found as in Equation (2.17), since all neccessary information about the nucleons is available in the simulation:

$$\epsilon_n = \frac{\sqrt{\langle r^2 \cos(n\phi)\rangle^2 + \langle r^2 \sin(n\phi)\rangle^2}}{\langle r^2 \rangle}. \tag{2.17}$$

Here r and ϕ are the polar coordinates of the nucleons in the frame in which the center of the distribution of wounded nucleons is located in the origin, and the average is taken over all wounded nucleons; n is the order. Eccentricity represents spatial anisotropy in azimuth. Spatial anisotropy causes momentum-space anisotropy, which is given by flow coefficients, v_n, which are a Fourier expansion of the single particle azimuthal distribution. The connection can be understood by imagining the fireball region produced in the collision as an ideal gas. It roughly has an elliptical shape. There is some pressure in the centre. The pressure drops an equal total amount along the major and minor axis moving from the centre and outwards. Since the minor axis is shorter, the pressure on the edge is greater than in the region at the end of the major axis. That makes the fireball expand faster in the direction of its minor axis.

It has been determined that the elliptic flow coefficient v_2 and ϵ_2 are correlated in the same way in hydrodynamic approaches [10] as in the string shoving model [9]).

3 Oxygen structure

Oxygen consists of 16 nucleons. It is hypothesized that nucleons in the oxygen nucleus are correlated, and form four α-clusters, conglomerations of two protons and two neutrons, which resemble an α-particle (Figure 3a). The α-particle is deeply bound and that is the reason it is often observed in nuclei, especially when the amount of neutrons and protons are equal, and are integer multiples of 2 [5]. The underlying reasons for the clustering in

light and medium sized nuclei is not the concern of this project, however. It rather explores the phenomenology of clustered nuclei.

Results from Variational Monte Carlo simulations [11, 12] can be closely reproduced if the nucleon positions are generated in clusters, according to the multivariate Gaussian distribution [3, 13]:

$$f_i(\boldsymbol{r}) = N \exp\Big(-\frac{3}{2}\Big(\frac{\boldsymbol{r} - \boldsymbol{\mu}_i}{r_c}\Big)^2\Big), \tag{3.1}$$

where $\boldsymbol{r}$ is the position of a nucleon centre, $\boldsymbol{\mu}_i$ is the coordinates of a cluster centre, r_c is a root mean square radius of the cluster and N is a normalisation constant. Cluster centres are located in the vertices of a tetrahedron with an edge length l_c. The optimal parameters for this model are $r_c = 1.1$ fm and $l_c = 3.2$ fm.

The model for α-clustered nuclei, described above, was implemented in Pythia as part of this project. An outline of the implementation is given in the following.

First the coordinates of cluster centers are randomly chosen. A random rotation matrix for each axis is then created, with angles from a uniform distribution from $-\pi$ to π. The rotation is applied to the coordinates of the cluster centres.

In the next step, the coordinates for each of the 16 nucleons are sampled from the normal distribution with standard deviation $\frac{r_c}{\sqrt{3}}$ and mean 0. For each set of four nucleons, constituting a cluster, the nucleon coordinates are translated by the vector given by the coordinates of one of the cluster centres. The first two nucleons of the set are assigned to be neutrons and the last two are protons.

Nucleon coordinates obtained from the newly implemented model are shown in Figure 3a. Next to it, coordinates generated using a Woods-Saxon distribution (Figure 3b) are shown for comparison.

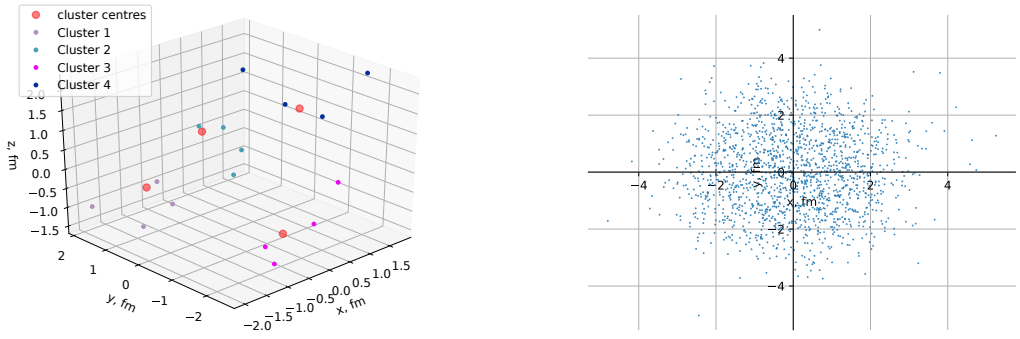

(a) (b)

Figure 3: Comparison of models. On figure (a), nucleon coordinates generated according to the model with clusters for one oxygen nucleus are shown. On figure (b) coordinates of nucleons from 100 nuclei generated using Woods-Saxon distribution are shown.

It is expected that the eccentricity of the collisions at very low and high centralities will differ little between the models. That would happen since high centralities correspond to edge collisions in which few nucleons participate. At low centralities the majority of the nucleons participate giving rounded fireball for both models. At mid-centrality, the eccentricity is expected to be lower for the implemented model, since there will be many events in which all the wounded nucleons belong to the same cluster. This gives a more rounded shape of the fireball in comparison to the one appearing in the collisions of nuclei that follow the Woods-Saxon distribution.

4 Results

4.1 Initial state quantities

We first study the distribution of distances between nucleons and the centre of the nucleus, and the distribution of distances between the nucleons, i.e. the 1 and 2 particle density distributions (Figure 4). It is mainly presented to demonstrate the basic differences between the nucleon distributions of the two models, and the results which follow immediately from them.

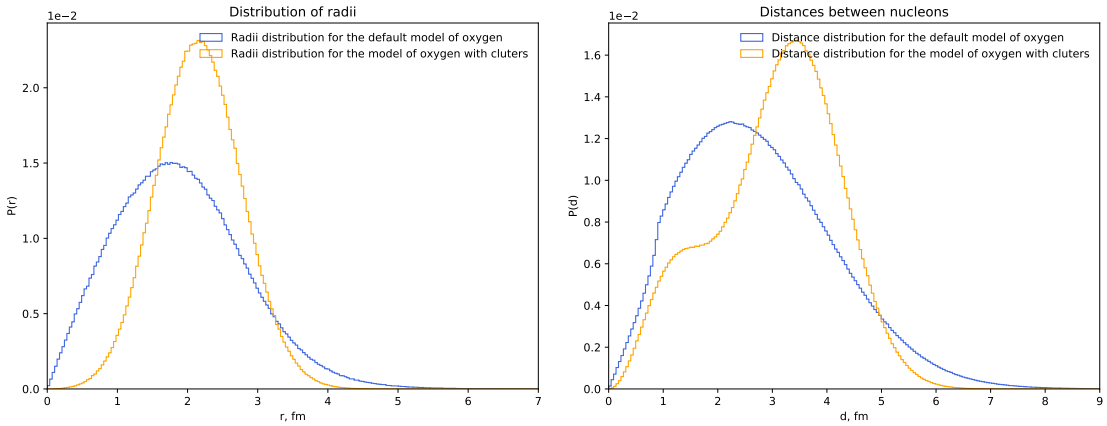

(a) (b)

Figure 4: Histograms for (a) the distances of nucleons from the centre of the nucleus and (b) the distances between the nucleons in the nucleus. Both are given for the default model of the oxygen using the Woods-Saxon distribution (blue) and the model of oxygen with clusters (orange).

The distribution of the distances of the nucleons to the centre (in the model with clusters, Figure 4a) is simply the distribution of a squared random variable from a Gaussian distribution with a non-zero mean. In the distribution of distances between the nucleons (model with clusters, Figure 4b), one can observe two "bumps". The one between 1 fm and 2 fm

gets its main contribution from the distances between the nucleons in the same cluster (24 possible pairs in one nucleus). The one from 3 fm to 4 fm gets its main contribution from the distances between the nucleons in different clusters (96 possible pairs). In contrast to that, the Woods-Saxon distribution shows no such behaviour.

The simulations were run with centre of mass energy per nucleon-nucleon collisions $\sqrt{s_{\mathrm{NN}}} =$ 8000 GeV.

The next studied initial state observable is the number of participants or wounded nucleons. As stated in subsection 2.3.1, this quantity has a direct impact on the number of produced particles. It was obtained by counting all the nucleons that interacted absorptively (Figure 5).

One can see that there is a larger probability for a collision to have a high number of participants when using the model with clusters, compared to the case of the default model. A plausible explanation is due to the fact that nucleon positions are correlated (nucleons are clustered together). This means that if a cluster is hit, all nucleons in the cluster are likely to be wounded. In the case of the Woods-Saxon distribution, there are most likely not many participating nucleons at the edges. The effect of this will be seen on the graphs with the comparison of the charged particle multiplicities (Figure 8), which shows the same pattern between the two models.

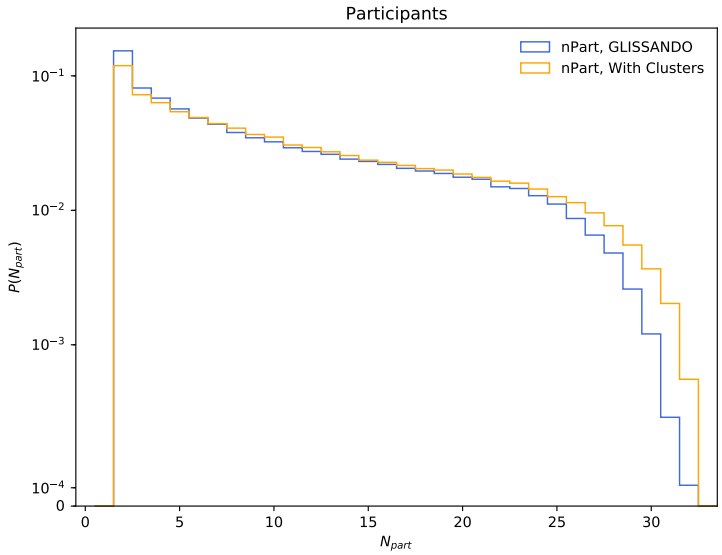

Figure 5: Histogram of the number of participants for the default model (blue) and the model with clustering (orange).

The spatial distribution of wounded nucleons affects both flow observables and the pseudorapidity distribution of the produced particles. To assess the former, the eccentricity is used. For each event the eccentricity was calculated using Equation (2.17). The averaged eccentricity for each centrality bin can be seen in Figure 6. The eccentricity distributions

for two bins where the models are significantly different (one where the average for the default model is greater, 50%-60% bin; and one where it is greater for the implemented model, 10%-20% bin) can be found on Figures 7a and 7b.

At centralities 70%-100%, corresponding to edge collision, there are 2-3 participants on average, so the result from the model including α-clusters is not significantly different from the original model. At centralities 60%-70%, 50%-60%, and 40%-50% there are 4.4, 6.1 and 8.2 participants on average. It can thus reasonably be assumed that wounded nucleons in such collisions come from the same cluster, giving lower eccentricity. Events with centralities 30%-40%, 20%-30% and 10%-20% have on average 10.8 and 14.4 and 18.5 participants respectively. In comparison to the more peripheral events, these events definitely have wounded nucleons belonging to different clusters. This explains why the eccentricity becomes larger in comparison to the default model. The last centrality bin has 24 participants on average meaning that the majority of the nucleons of both nuclei are wounded.

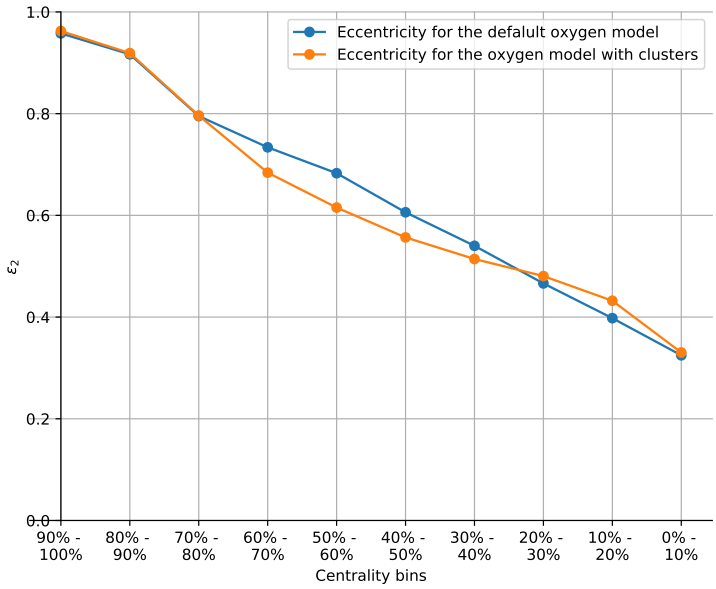

Figure 6: Eccentricity comparison for the default model (blue) and the model with clustering (orange) in centrality bins.

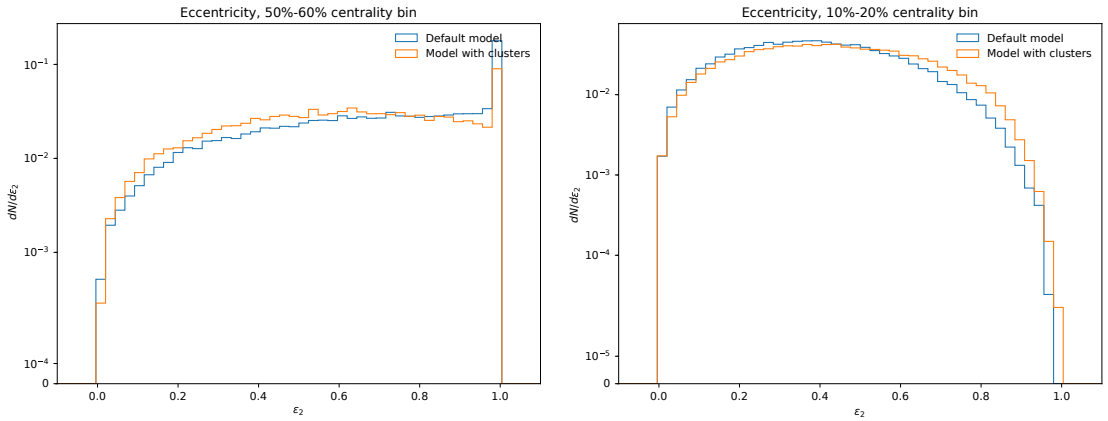

(a) (b)

Figure 7: Eccentricity distributions for a 50%-60% centrality bin (a) and a 10%-20% centrality bin (b) for the default model (blue) and the model with clustering (orange)

One can notice that there is a sharp spike on figure 7a at the eccentricity close to 1. Such events correspond to the cases where there are only 2 participants, which incidentally give high eccentricity.

4.2 Particle level results

As a first important final state observable, histograms showing the distribution of the events with a given number of particles detected in the central (Figure 8a) and forward (Figure 8b) regions, with $|\eta| < 0.5$ and $3.5 < |\eta| < 5$ respectively, were obtained.

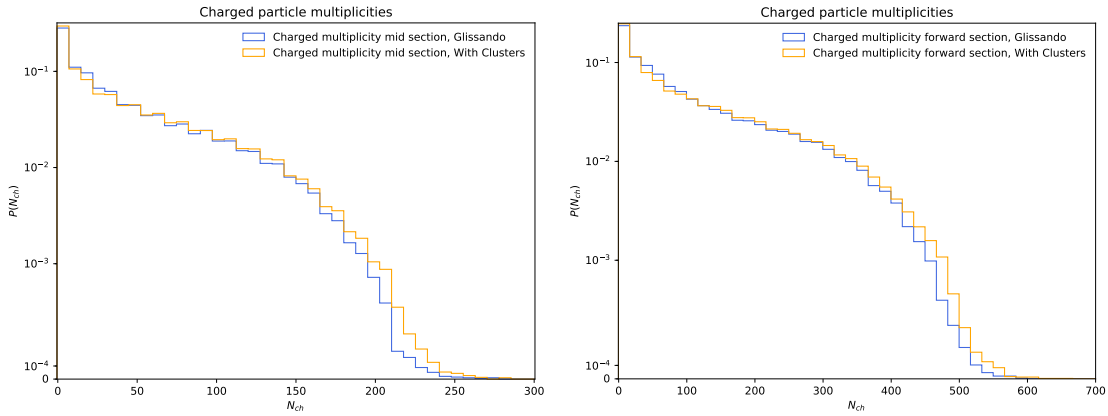

(a) (b)

Figure 8: Charged particle multiplicity in the central (a) with pseudorapidity $\eta < 0.5$, and forward (b) with $3.5 < \eta < 5$, regions for the default model of oxygen (blue) and the model of oxygen with clusters (orange).

As stated before, in Subsection 2.4, the charged particle multiplicity in the forward region (on Figure 8b) can be used to divide the events into centrality bins. The multiplicity monotonically depends on the impact parameter and is large when the impact parameter is small and small when the impact parameter is large. Let $f(x)$ be the multiplicity distribution and X be the measured multiplicity in an event. To determine which centrality the event belongs to, one should calculate the integral

$$c = \frac{1}{N} \int_X^\infty f(x)dx,$$

where N is a normalisation constant. Effectively, binning the events by centrality can be done just by finding 10 quantiles of the particle multiplicity distribution.

The pseudorapidity distributions of produced particles as a function of centrality can now be found (Figure 9). For that, more collisions were simulated and the information about particle pseudorapidity was retrieved, as well as the charged particle multiplicity in the forward region. The data from each event was used to fill different histograms depending on which centrality bin the event belongs to.

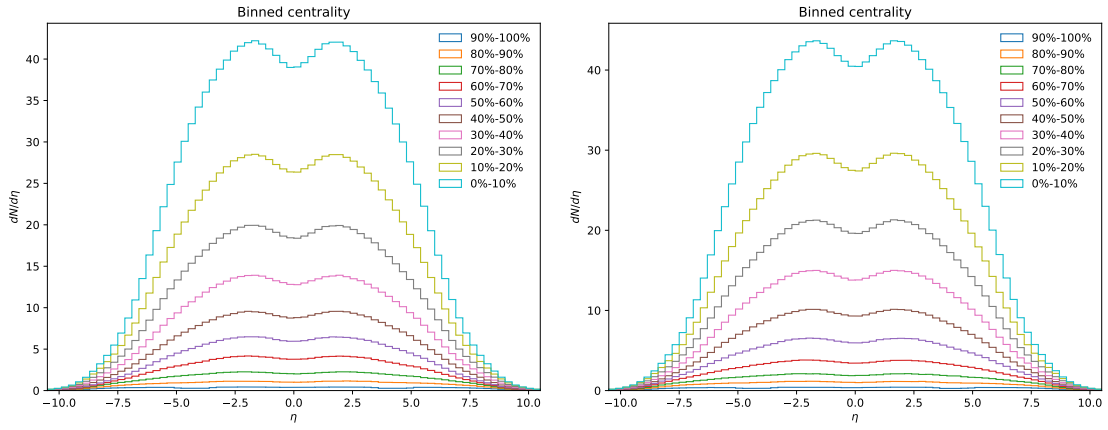

(a) (b)

Figure 9: The pseudorapidity distributions of produced particles in centrality bins for the default model (a) and the model with clusters (b).

One can see in Figures 9a and 9b, that the number of particles in a single event is higher at lower centralities of the collision.

The differences between Figures 9a and 9b are easier to observe by taking the ratio of the two. The plot on Figure 10 was obtained by taking a ratio of the values from the model with clusters, to the ones from the model that uses the Woods-Saxon distribution. It is noticeable that, except for the highest centralities, the model with clusters has more particles produced in the forward region than in the central region. That is most likely due to the increased number of secondary collisions, since nucleons in the clusters are located tighter and the clusters may overlap.

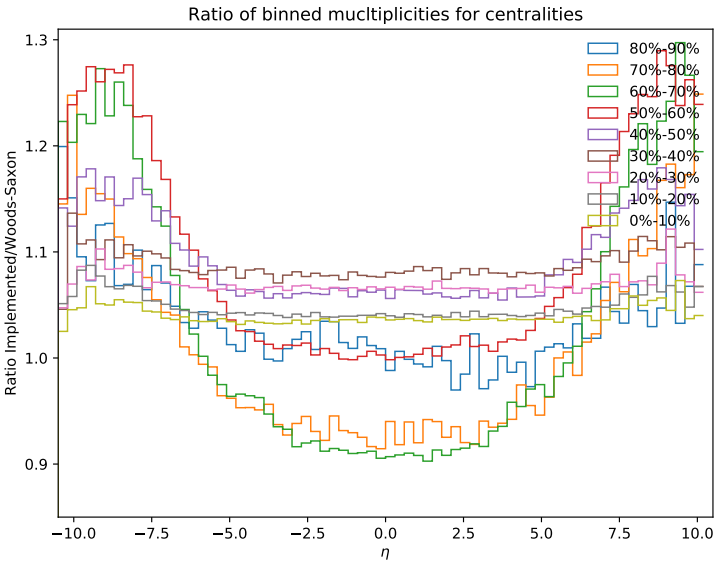

Figure 10: Ratio of $\frac{dN}{d\eta}$ for the implemented model to the value obtained using default model for different centrality bins.

5 Conclusion

The LHC has planned to dedicate a run for high energy $^{16}O^{16}O$ collisions, to see the effects of the exotic geometry of oxygen nuclei and to resolve some questions in cosmic ray physics. Its nucleons are organised in four α-clusters. During this project a model that reproduces this structure of oxygen was implemented in Pythia. Also, some of the basic observables, which will be studied early in the experiment, were investigated. Among the main observations is that collisions generated have a slightly higher probability for a larger number of participants than the default model. Consequently, the former have a higher multiplicity of charged particles. Also in the new model, most events have lower eccentricity, and the production of particles is more shifted to the forward rapidity.

References

[1] N. Summerfield, B.-N. Lu, C. Plumberg, D. Lee, J. Noronha-Hostler, and A. Timmins, "^{16}O ^{16}O collisions at energies available at the BNL Relativistic Heavy Ion Collider and at the CERN Large Hadron Collider comparing α clustering versus substructure," *Phys. Rev. C* **104** (2021), no. 4 L041901, 2103.03345.

[2] J. Brewer, A. Mazeliauskas, and W. van der Schee, "Opportunities of OO and pO collisions at the LHC," in *Opportunities of OO and pO collisions at the LHC*, 3, 2021. 2103.01939.

[3] P. Bożek, W. Broniowski, M. Rybczynski, and G. Stefanek, "GLISSANDO 3: GLauber Initial-State Simulation AND mOre..., ver. 3," *Comput. Phys. Commun.* **245** (2019) 106850, 1901.04484.

[4] T. Sjöstrand, S. Ask, J. R. Christiansen, R. Corke, N. Desai, P. Ilten, S. Mrenna, S. Prestel, C. O. Rasmussen, and P. Z. Skands, "An introduction to PYTHIA 8.2," *Comput. Phys. Commun.* **191** (2015) 159–177, 1410.3012.

[5] T. A. Lähde and U.-G. Meißner, *Nuclear Lattice Effective Field Theory: An introduction*, vol. 957. Springer, 2019.

[6] M. L. Miller, K. Reygers, S. J. Sanders, and P. Steinberg, "Glauber modeling in high energy nuclear collisions," *Ann. Rev. Nucl. Part. Sci.* **57** (2007) 205–243, nucl-ex/0701025.

[7] C. Bierlich, G. Gustafson, L. Lönnblad, and H. Shah, "The Angantyr model for Heavy-Ion Collisions in PYTHIA8," *JHEP* **10** (2018) 134, 1806.10820.

[8] A. Buckley *et. al.*, "General-purpose event generators for LHC physics," *Phys. Rept.* **504** (2011) 145–233, 1101.2599.

[9] C. Bierlich, S. Chakraborty, G. Gustafson, and L. Lönnblad, "Setting the string shoving picture in a new frame," *JHEP* **03** (2021) 270, 2010.07595.

[10] H. Niemi, G. S. Denicol, H. Holopainen, and P. Huovinen, "Event-by-event distributions of azimuthal asymmetries in ultrarelativistic heavy-ion collisions," *Phys. Rev. C* **87** (2013), no. 5 054901, 1212.1008.

[11] D. Lonardoni, A. Lovato, S. C. Pieper, and R. B. Wiringa, "Variational calculation of the ground state of closed-shell nuclei up to $A = 40$," *Phys. Rev. C* **96** (2017), no. 2 024326, 1705.04337.

[12] E. Buendia, F. J. Galvez, and A. Sarsa, "Projected multicluster model with Jastrow and linear state dependent correlations for 12 <= A <= 16 nuclei," *Phys. Rev. C* **70** (2004) 054315, nucl-th/0405027.

[13] M. Rybczyński, M. Piotrowska, and W. Broniowski, "Signatures of α clustering in ultrarelativistic collisions with light nuclei," *Phys. Rev. C* **97** (2018), no. 3 034912, 1711.00438.